Self-Assembly of Coil/Liquid-Crystalline Diblock Copolymers in a Liquid Crystal Solvent

Neal R. Scruggs,[†] Rafael Verduzco,[†] David Uhrig,[‡] Waliullah Khan,[§] Soo-Young Park,[§] Jyotsana Lal,[||] and Julia A. Kornfield*,[†]

Division of Chemistry and Chemical Engineering, California Institute of Technology, 1200 California Boulevard, Pasadena, California 91125, Center for Nanophase Materials Sciences, Oak Ridge National Laboratory, One Bethel Valley Road, Oak Ridge, Tennessee 37831, Department of Polymer Science, Kyungpook National University, 1370 Sangyuk-dong, Buk-gu, Daegu 702-701, Korea, and Intense Pulsed Neutron Source, Argonne National Laboratory, 9700 South Cass Avenue, Argonne, Illinois 60439

Received July 16, 2008; Revised Manuscript Received October 18, 2008

ABSTRACT: Diblock copolymers having a random-coil polymer block (polystyrene, PS) connected to a side-group liquid crystal polymer (SGLCP) self-assemble in a nematic liquid crystal (LC), 4-pentyl-4′-cyanobiphenyl, into micelles with PS-rich cores and SGLCP-rich coronas. The morphologies of block copolymers with varying PS content are characterized as a function of temperature and concentration using small-angle neutron scattering, rheometry, and transmission electron microscopy. Unlike conventional solvents, the nematic LC can undergo a first-order transition between distinct fluid phases, accessing the regimes of both strong and slight selectivity in a single polymer/solvent pair. Micelles dissolve away above a microphase separation temperature (MST) that is often equal to the solution's isotropization point, T_{NI}. However, increasing or decreasing the polymer's PS content can shift the MST to be above or below T_{NI}, respectively, and in the former case, micelles abruptly swell with solvent at T_{NI}. Comparable effects can be achieved by modulating the overall polymer concentration.

Introduction

It is well-known that linear diblock copolymers in the melt can self-assemble into a variety of morphologies (e.g., spheres, cylinders, and lamellae), depending on the thermodynamic incompatibility between the two blocks.[1] The block copolymer's equilibrium structure is determined by the overall degree of polymerization, the relative fractions of *A* and *B* blocks, and the Flory−Huggins interaction parameter, χ_{AB}, which quantifies primarily enthalpic interactions between the blocks.[2] In solution, the range of accessible microstructures for a given a diblock copolymer can be expanded through modulation of the solvent's "selectivity", characterizing its relative compatibility with the *A* and *B* blocks: a good solvent for block *A* is defined as strongly selective, slightly selective, or neutral if it is, respectively, a nonsolvent, marginal solvent, or good solvent for block *B*.[3−10] Micelles typically form in dilute solutions with a strongly or slightly selective solvent.[4,5,7] The additional contributions of polymer/polymer interactions with increasing concentration can lead to a rich phase behavior of micelles with various shapes, sizes, and types of long-range order,[3−5,7−9] even in neutral solvents.[4,6,10]

Thermodynamic compatibility between polymers and solvents is typically a monotonic function of temperature, but in contrast to conventional solvents, small-molecule liquid crystals (LCs) can undergo discontinuous, first-order phase transitions between distinct fluid mesophases with substantially different thermodynamic properties. The simplest of these liquid crystalline mesophases is termed the "nematic" phase[11] and is characterized by molecules that diffuse freely but tend to retain orientation in a preferred direction called the "director." Their orientational order makes nematic LCs poor solvents for random-coil polymers, but upon heating to the isotropic phase, the two may become completely miscible.[12−14] Side-group liquid crystal polymers (SGLCPs) have mesogenic moieties laterally attached to the polymer backbone, which can make them compatible with LC solvents in both the nematic and the isotropic phases.[12,15−24]

One might expect diblock copolymers that join a random-coil block with an SGLCP block to have unique phase behavior when dissolved in an LC because the solvent's selectivity can change abruptly at a phase transition. Block copolymers coupling random-coil polymers to SGLCPs have been extensively studied in the bulk,[25−30] but to our knowledge, only the Finkelmann group investigated self-assembly of such polymers in LC solvent[31−34] prior to our group's reports.[12,35−38] These systems are interesting from a practical standpoint because swelling random-coil/SGLCP block copolymers with small-molecule solvent increases the strength and speed of the polymers' responses to electromagnetic stimuli, making them better candidates for use in devices such as liquid crystal displays.[35]

To gain a better understanding of the thermodynamics governing self-assembly of coil/SGLCP diblock copolymers in a nematic solvent, we have synthesized a library of polymers in which the relative proportions of the two blocks is varied keeping the overall molecular weight fixed. We dissolve these in a small-molecule LC and use small-angle neutron scattering, rheometry, and transmission electron microscopy to characterize the self-assembled microstructure as a function of temperature and polymer concentration. In comparison to conventional solvents, our results demonstrate that the LC's selectivity is uniquely sensitive to temperature, often changing from strongly selective to neutral or slightly selective directly upon isotropization.

Experimental Section

Materials. Side-group liquid crystal polymers (SGLCPs) were synthesized by polymer analogous chemistry. Mesogenic side groups were attached via a siloxane linking group to an existing polymer backbone containing 1,2-butadiene in a platinum-catalyzed hydrosilylation reaction with the pendant vinyl moieties. Using this

* To whom correspondence should be addressed. E-mail: jak@cheme.caltech.edu.
[†] California Institute of Technology.
[‡] Oak Ridge National Laboratory.
[§] Kyungpook National University.
[||] Argonne National Laboratory.

10.1021/ma801598y CCC: $40.75
Published on Web 12/05/2008

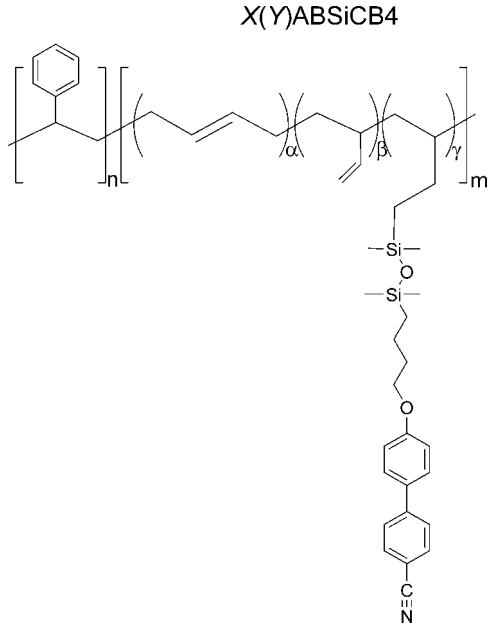

Figure 1. Chemical structure of the side-group liquid crystal polymers. Diblock copolymers have a coil block composed of polystyrene and the SGLCP homopolymer has $n = 0$. The polymers' names are derived from the molecular weights of the liquid crystal polymer block, *X*, and the coil block, *Y*, in units of kg/mol, the letters "AB" or "H" indicate a diblock copolymer or homopolymer, respectively. In addition to monomers having an attached mesogen, the polymers also contain some residual 1,2- and 1,4-butadiene monomers. Compositions, expressed as the mole fractions α, β, and γ, are given in Table 1.

strategy, the same prepolymer can be functionalized with different mesogens to compare SGLCPs having different side groups but identical degrees of polymerization. The SGLCP's polydispersity, molecular weight, and architecture are defined during the prepolymer synthesis, allowing one to take advantage of the versatility and control afforded by anionic polymerization.

Coil/SGLCP diblock copolymers were synthesized from poly[styrene-*b*-1,2 butadiene] (PS-PB). A series of four PS-PB diblocks having approximately equally sized PB blocks ($M_n \approx 55$ kg/mol) and variably sized PS blocks (from 40 to 120 kg/mol) was prepared by anionic polymerization using sequential monomer addition, with 1,2-bis(piperidino)ethane added during the butadiene polymerization.[39−41] The PB block contains greater than 95 mol % 1,2-butadiene monomers, the remainder being unreactive 1,4-butadiene. The sizes of the PS and PB blocks were chosen based on a prior PS-SGLCP-PS triblock copolymer,[35−38] here using the change in PS block length to probe both lower and greater PS block lengths than examined previously. The diblock copolymer products were characterized in terms of molecular weight and molecular weight distribution by using SEC-RI and SEC-LS, in THF (employing a Waters Alliance 2695 Separations Module and 3 PL Mixed-C Ultrapolystyragel columns at 35 °C, equipped with Waters 2414 RI detector and Wyatt Minidawn LS detector); the materials were further characterized for composition and microstructure of polybutadiene by using SEC-UV (Waters 2996 UV detector) and ^{1}H NMR in deuterochloroform (Varian 500 MHz).

This library of PS-PB diblocks was used to synthesize a series of PS-SGLCP diblock copolymers (Figure 1) having side groups attached "end-on", with the mesogen's long axis perpendicular to the polymer backbone. We have previously reported the details of the side-group's synthesis and attachment,[36] and the polymers' properties are summarized in Table 1. In addition to the diblocks, a complementary SGLCP homopolymer was synthesized by attaching mesogenic side groups to an anionically polymerized 1,2-PB homopolymer ($M_n = 47.5$ kg/mol) purchased from Polymer Source (Montreal, Quebec). Its molecular weight was chosen to closely match that of the diblocks' SGLCP blocks and its properties are also summarized in Table 1.

An additional set of diblocks and an analogous homopolymer was synthesized from the same set of prepolymers using a different mesogenic side group. Synthesis and analysis of these "side-on" polymers is described in the Supporting Information.

Gel permeation chromatography (GPC) and proton NMR were used to characterize the polymers after side-group attachment. The polymers' polydispersities were measured by GPC using four, 30 cm analytical gel columns (Polymer Laboratories PLgel, 10 μm) connected in series and a Waters 410 differential refractometer with tetrahydrofuran (THF) as the mobile phase. The system was calibrated with a series of monodisperse polystyrene standards and the polydispersity index (PDI $= M_w/M_n$) was calculated from the GPC trace using Waters's Millenium software. Proton NMR spectra were recorded from solutions of the polymers in $CDCl_3$ on a 300 MHz Varian NMR spectrometer and used to calculate the degree of conversion of the SGLCP block. The percentage of reacted 1,2-butadiene monomers was calculated from the relative intensities of peaks at $\delta = 4.9$ ppm (characteristic of vinylic hydrogens in 1,2-butadiene) and $\delta = 3.9$ ppm (characteristic of alkyl hydrogens adjacent to the side group's cyanobiphenyl core). The percentage of 1,4-butadiene monomers in the SGLCP block was assumed unchanged from the prepolymer.

Solutions of SGLCP homopolymers or coil-SGLCP diblock copolymers in liquid crystal solvent were prepared by dissolving a polymer together with the nematic LC 4-pentyl-4′-cyanobiphenyl (5CB) in dichloromethane, then evaporating the dichloromethane under a stream of air followed by drying in vacuum for at least 18 h.

Methods. The transition temperatures of polymer/LC solutions were measured by polarized optical microscopy (POM). A drop of solution was placed on a microscope slide and observed between crossed polarizers in a Zeiss Universal stereomicroscope with temperature controlled by a Mettler FP82 hot stage. While heating at a rate of 1 °C/min, the temperature at which the colorful, birefringent texture began to disappear was recorded as the isotropization point, T_{NI}. Two temperatures were recorded for samples that became biphasic during the transition: the temperature at which the first black spots appear marks the beginning of the biphasic region and the temperature at which the last colorful spots disappear marks the end.

For the purpose of imaging using transmission electron microscopy (TEM), drops of solutions containing 1 wt % polymer dissolved in 5CB were allowed to spread on distilled water at 40 °C. The volume of 5CB/polymer solution was approximately 15 μL and the area of the water was 110 mm^2; therefore, the LC layer floating on the water was approximately 12 μm thick. Neither 5CB nor the coil-SGLCP polymer has appreciable solubility in water. A specimen of this LC/polymer solution was picked up on a carbon-coated grid, dried at ambient conditions for 3 to 4 h, and then exposed to RuO_4 vapor for 10 min. The specimens were imaged using a Hitachi H-7600 transmission electron microscope operating at 100 kV.

Rheometry was performed on solutions of diblock copolymers dissolved in 5CB using a TA Instruments ARES-RFS fluids rheometer with a dynamic range of 1×10^{-3} rad/s $\leq \omega \leq 2 \times 10^2$ rad/s. Approximately 200 mg of solution was held in a titanium cone-and-plate tool 25 mm in diameter. The temperature was controlled with the rheometer's built-in Peltier device and was stable to within 0.1 °C. Prior to beginning each experiment, the sample's thermal history was erased by heating it to 60 °C for at least 5 min, then annealing at the desired temperature for at least 5 min. Frequency sweeps were performed in the linear regime at temperatures ranging from 25 °C to at least 60 °C, traversing 1 °C temperature increments near the isotropization point. The strain amplitude (approximately 5% for most samples) was selected to optimize the torque while ensuring all measurements were made in the linear viscoelastic regime. Temperature ramps up to 60 °C

Table 1. Molecular Weight, Conversion, and Polydispersity of the Liquid Crystalline Polymers

	PS Block	SGLCP Block				
name	M_n [kg/mol]	M_n [kg/mol]	mole fraction 1,2-PB	mole fraction 1,4-PB	mole fraction LC	PDI[a]
350HSiCB4		347	0	0.11	0.89	1.27
470(40)ABSiCB4	43	472	0	0.01	0.99	1.19
390(60)ABSiCB4	59	388	0.15	0.03	0.85	1.11
420(80)ABSiCB4	83	422	0.05	0.05	0.90	1.07
320(120)ABSiCB4	121	323	0.22	0.01	0.77	1.05

[a] PDI = polydispersity index (M_w/M_n).

were performed in the linear regime with $\omega = 10$ rad/s at a heating rate of 1 °C/min.

Time-of-flight small angle neutron scattering (SANS) experiments were performed on the Small-Angle Scattering Instrument (SASI) at Argonne National Laboratory's Intense Pulsed Neutron Source (IPNS). The instrument records intensity at scattering vectors, $|\boldsymbol{q}| = q = 4\pi/\lambda \sin(\theta/2)$, of approximately 6.7×10^{-3} Å^{-1} $\leq q \leq 2.0$ Å^{-1}. To achieve sufficient neutron scattering contrast, polymers were dissolved in perdeuterated 5CB (d_{19}5CB) that was synthesized according to published methods.[15,42] The nematic−isotropic transition temperature, T_{NI}, of d_{19}5CB is approximately 3 °C lower than that of hydrogenated 5CB.[42] SANS and rheometry are brought into registration with one another by comparing results at the same reduced temperature, $T-T_{NI}$. In samples exhibiting biphasic regions, temperatures were reduced relative to the phase transition's initial onset temperature during heating (Supporting Information, Table S1).

Solutions of diblock copolymers in d_{19}5CB were contained in cells consisting of circular quartz windows spaced apart by a quartz ring 1.0 mm thick. Samples were loaded in the polydomain state; no effort was made to achieve uniform alignment of the liquid crystal director. During the scattering experiments the cells were held in a heated aluminum block where the temperature was stable within approximately 0.1 °C. At least fifteen minutes of temperature equilibration was allowed prior to collecting data. Samples were typically irradiated for one hour and the two-dimensional scattering pattern was circularly averaged to yield data in the form of intensity versus q. In rare instances where insufficient sample quantities prevented us from filling the cells completely, the scattering patterns were shifted vertically so as to overlap at high q with an analogous polymer solution of equal concentration.

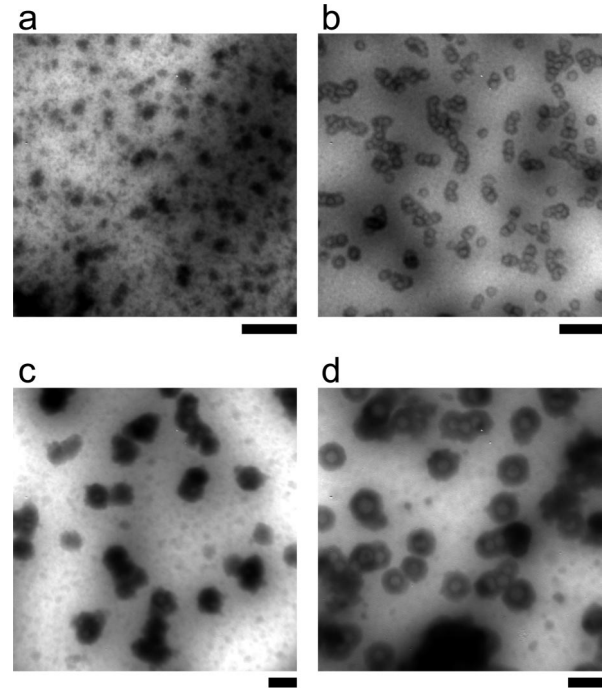

Figure 2. TEM micrographs of 1 wt % solutions of (a) 470(40)ABSiCB4, (b) 390(60)ABSiCB4, (c) 420(80)ABSiCB4, and (d) 320(120)ABSiCB4 in 5CB, stained with RuO_4. The scale bars below each image correspond to 500 nm.

Results

TEM micrographs of diblock copolymers dissolved in 5CB are consistent with self-assembly into micelles composed of PS-rich cores surrounded by SGLCP-rich coronas (Figure 2). The samples were treated with RuO_4, a compound used to stain phenyl rings, which are present both in the PS and SGLCP block, as well as the solvent 5CB. Core−shell micellar structures were observed for all but the shortest PS block length (Figure 2b, c, and d), while micrographs from solutions of 470(40)ABSiCB4 feature dark spots without clearly identifiable cores (Figure 2a). The overall diameters of the core−shell structures measured directly from the micrographs of 390(60)ABSiCB4, 420(80)ABSiCB4, and 320(120)ABSiCB4 (with N = the number of micelles averaged) are $d = 120 \pm 20$ nm ($N = 167$), $d = 420 \pm 50$ nm ($N = 27$), and $d = 420 \pm 50$ nm ($N = 31$), respectively. These provide useful estimates of the micelle diameters, but uncertainties related to staining artifacts, sample preparation, and the small size of the sampled population limit our ability to draw quantitative conclusions from this data.

Nevertheless, the TEM micrographs do suggest that PS-SGLCP micelles are larger than those typically formed by conventional asymmetric block copolymers in solution, which are typically 10−100 nm in size (for examples see refs 5, 6, 45). Most studies are restricted to diblocks with molecular weights less than 100 kg/mol, which immediately suggests one factor that might contribute to the comparatively large size of our micelles: our polymers are nearly five times larger. Indeed, the large domain sizes observed here are more consistent with the approximately 325 nm structures observed in solutions of ultrahigh molecular weight (3600 kg/mol) PS−PI diblocks in neutral or selective solvents.[43] However, we note that without detailed knowledge of our micelles' sizes and shapes, or the partitioning of solvent between the core and corona, we cannot confidently make comparisons to other diblock copolymer systems.

The neutron scattering patterns from diblock copolymer solutions all have a few basic features in common (Figure 3 and Figure 4). The scattered intensity is highest at low q and drops precipitously as q increases, until it merges with $I(q)$ of the equivalent SGLCP homopolymer for q greater than approximately 0.06 Å^{-1}. At large q, q-independent, incoherent background scattering becomes dominant beyond $q \approx 0.3-0.5$ Å^{-1}. The magnitude of the scattered intensity at low q is highly sensitive to changes in temperature (Figure 3). For example, the maximum intensity, I_{max}, for a 5 wt % 320(120)ABSiCB4 solution drops an order of magnitude as the temperature is raised from T_{NI} −8 °C to T_{NI} +7 °C (Figure 3a). A similar decrease of I_{max} is observed as 10 wt % 320(120)ABSiCB4 is heated from T_{NI} −8 °C to T_{NI} +17 °C and then drops down to the level seen for the equivalent SGLCP homopolymer as T increases to T_{NI} +27 °C (Figure 3b). At high q ($q > \approx 0.06$ Å^{-1}), however, $I(q)$ is insensitive to temperature (Figure 3). The high-q scattering is also unaffected by changing the size of the polystyrene block (Figure 4). Scattering patterns from diblocks having approximately matched SGLCP blocks and PS blocks

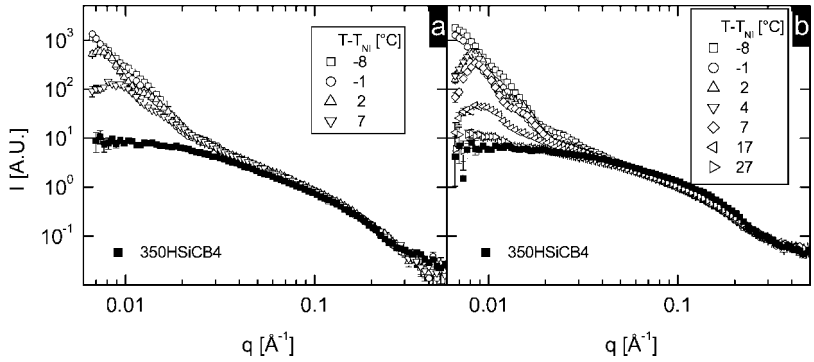

Figure 3. SANS patterns from solutions of (a) 5 wt % 320(120)ABSiCB4 and (b) 10 wt % 320(120)ABSiCB4 in d_{19}5CB at a variety of temperatures (open symbols) as compared to patterns from their analogous homopolymer solutions collected at $T = T_{NI} + 16.5$ °C (closed symbols). The low-q scattering of the diblock solutions is shown in detail in Figures 5 and 6.

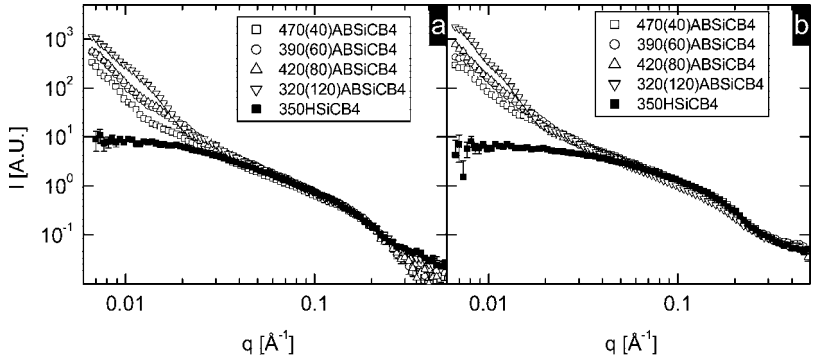

Figure 4. SANS patterns from solutions of (a) 5 wt % and (b) 10 wt % solutions of diblock copolymers in d_{19}5CB at $T \approx T_{NI} - 9$ °C (open symbols) as compared to patterns from their analogous homopolymer solutions collected at $T = T_{NI} + 16.5$ °C (closed symbols). The low-q scattering of the diblock solutions is shown in detail in Figures 5 and 6.

varying in size from 40 to 120 kg/mol all overlap with the equivalent SGLCP homopolymer at q greater than approximately 0.06 Å^{-1} (Figure 4).

Because the high-q scattering is completely described by the scattering of SGLCP homopolymers (Figures 3 and 4), this portion of the SANS pattern is attributed to the monomer-level structure of SGLCP chains. At low values of q, the self-assembled structure dominates the scattering and from here on the presentation of SANS patterns will be restricted to this regime. The micelles are large ($d > 100$ nm estimated by TEM) compared to the range of q accessible in our SANS experiment: the minimum accessible q is $q_{min} = 0.007$ Å^{-1}, revealing structures on length scales of 90 nm or less. *This precludes fitting* our SANS data to theoretical models for micelle structures. Nevertheless, significant qualitative conclusions may be drawn from the scattering data. Specifically, the changes in the SANS pattern show structural transitions between one micellar state to another and from micelles to dissolved chains.

We believe that the micellar dispersions studied here are in the "liquid-like" concentration regime,[3] due to the absence of either structure factor peaks (intermicelle interference)[3,8] or diffraction peaks (micellar lattices).[44,45] However, the presence of such features at $q < q_{min}$ cannot be excluded.

The end-on diblock copolymers 470(40)ABSiCB4, 390(60)ABSiCB4, 420(80)ABSiCB4, and 320(120)ABSiCB4 comprise a series with approximately constant total molecular weight (440−510 kg/mol) having increasing PS content from 8 to 23 wt % (Table 1). The structural characteristics of the SANS patterns (Figure 5a−d and Figure 6a−d) change and the overall strength of scattering decreases in the vicinity of the transition from the nematic phase (open symbols) to the isotropic phase (filled symbols), coinciding with the temperature range over which the elastic character that is evident at low temperature decreases during heating (Figure 5e−h and Figure 6e−h). These trends accord with the fact that the nematic phase of the solvent is highly selective and the isotropic phase is capable of dissolving both PS and the SGLCP.

At a concentration of 5 wt %, all four block copolymers share certain overall features at temperatures well below T_{NI}: similar strength of scattering at low q, monotonic decrease in $I(q)$ with q, and similar storage moduli ($G' \approx 2$ Pa) to each other. With increasing temperature, there are some interesting differences in the way that order and elasticity are lost. The polymer with the shortest PS block passes through a biphasic window of temperature just above T_{NI}; the enhancement of the storage modulus observed in the biphasic region (peak between dashed lines in Figure 5e) is consistent with the known contribution of liquid−liquid interfaces to the elasticity of two-phase liquids. Otherwise, the effect of temperature on the viscoelastic properties of the diblocks with polystyrene molecular weights, M_{PS}, of 40, 60, and 80 kg/mol are quite similar: G' drops from $G' > 2$ Pa when they are fully nematic to $G' < 0.03$ Pa when they are fully isotropic, and $|\eta^*|/\eta_{5CB}$ changes from being greater than 10 and frequency dependent, to being less than 10 and frequency independent (Figure 7). This loss of elasticity is accompanied by a decrease in the maximum scattered intensity (Figure 5a−c, inset). Unlike the other three diblocks, the 5 wt % solution of the polymer with the longest PS block ($M_{PS} =$ 120 kg/mol) retains significant elasticity even when completely isotropic ($G' > 0.03$ Pa up to $T_{NI} + 5$ °C, Figure 5h). Correlated with the observed elasticity in the isotropic phase, the SANS pattern shows that the transition from the nematic to the isotropic phase produces an order−order transition: at a temperature just above T_{NI}, $I(q)$ shows considerable structure and the maximum intensity remains substantial (Figure 5d). The correlated changes in SANS and G' are similar to those observed at the

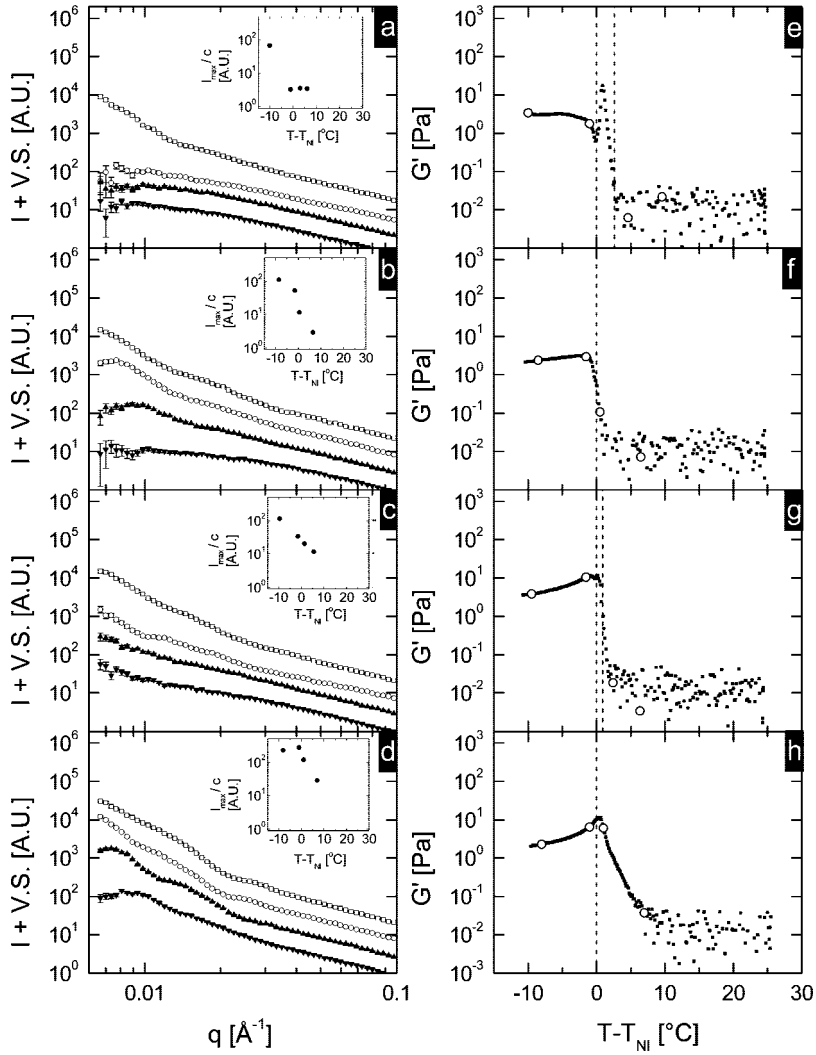

Figure 5. SANS and rheology of 5 wt % diblock copolymer solutions proceeding from top to bottom in order of increasing PS block length. The low-q portion of SANS patterns collected in the nematic phase (open symbols) and the isotropic phase (closed symbols) (a-d) is plotted alongside the storage modulus, $G'(\omega = 10$ rad/s), as a function of temperature upon heating a rate of 1 °C/min (d−h). SANS patterns were collected at the following reduced temperatures: $T - T_{NI}$ = (a) −10.2 °C (□), −1.2 °C (○), 1.8 °C (▲), and 4.8 °C (▼); (b) = −8.4 °C (□), −1.4 °C (○), 0.6 °C (▲), and 6.6 °C (▼); (c) = −9.5 (□), −1.5 °C (○), 1.5 °C (▲), and 5.5 °C (▼); and (d) = −8.0 °C (□), −1.0 °C (○), 1.0 °C (▲), and 7.0 °C (▼). Patterns are successively shifted upward from the highest temperature by factors of three for clarity. For parts (d−h), white circles indicate the same reduced temperatures at which SANS patterns were collected and dashed lines indicate the beginning and end of the nematic−isotropic transition.

order−disorder or order−order transition temperatures of non-LC diblock copolymers in isotropic solvents.

The temperature at which the low-q scattering decreases to the level seen in an analogous homopolymer solution increases with increasing PS block length. In the case of the smallest PS block ($M_{PS} = 40$ kg/mol) this temperature is below T_{NI} (Figure 5a); for the next in the series ($M_{PS} = 60$ kg/mol), it is above T_{NI} (at $T_{NI} + 6.6$ °C, $I(q)$ is similar to that of a homopolymer solution; Figure 5b). For PS block lengths greater than 60 kg/mol, 5 wt % solutions show greater scattering than their SGLCP hompolymer counterparts even at the highest temperatures tested; and the scattering that remains at $T - T_{NI} > 5$ °C is of higher intensity for the polymer with $M_{PS} = 120$ kg/mol (Figure 5d) than for the polymer with $M_{PS} = 80$ kg/mol (Figure 5c).

Similarly, the temperature at which G' drops below 1 Pa increases with increasing PS block length. For the diblocks with $M_{PS} = 40$ kg/mol, G' falls to 1 Pa at $T_{NI} - 0.5$ °C (Figure 5e). When $M_{PS} = 60$ or 80 kg/mol, G' falls to 1 Pa or lower at the end of the nematic−isotropic phase transition (Figure 5f and g). For the longest PS block in the series ($M_{PS} = 120$ kg/mol), the decrease in G' with increasing temperature beyond T_{NI} is relatively gradual, reaching 1 Pa at a temperature distinctly greater than T_{NI} (Figure 5h). Within the nematic phase, increasing PS block length causes the temperature dependence of G' to change from softening ($M_{PS} = 40$ kg/mol) to stiffening ($M_{PS} = 60$, 80, and 120 kg/mol), and the steepness of the stiffening with temperature increases with the size of the PS block for $M_{PS} = 60-120$ kg/mol (Figure 5e−h).

Solutions of 10 wt % diblock copolymer (Figure 6) exhibit similar trends in SANS and rheology as the 5 wt % solutions. At high q, the scattered intensity is approximately two times greater in the 10 wt % solutions as in their 5 wt % counterparts, as it should be for scattering arising from approximately the monomer-level structure. Interestingly, at small q, the 10 wt % solutions with $M_{PS} \leq 60$ kg/mol do *not* have greater intensity; indeed, when normalized by concentration, I_{max}/c is greater for the 5 wt % solutions in each pair. When $M_{PS} \geq 80$ kg/mol, I_{max}/c is approximately the same for 5 and 10 wt % solutions, as expected. For 10 wt % solutions, the magnitude of the storage modulus is approximately 10 times greater than its 5 wt % counterpart. The former is consistent with an approximate contribution of kT per corona chain, as expected for overlapping

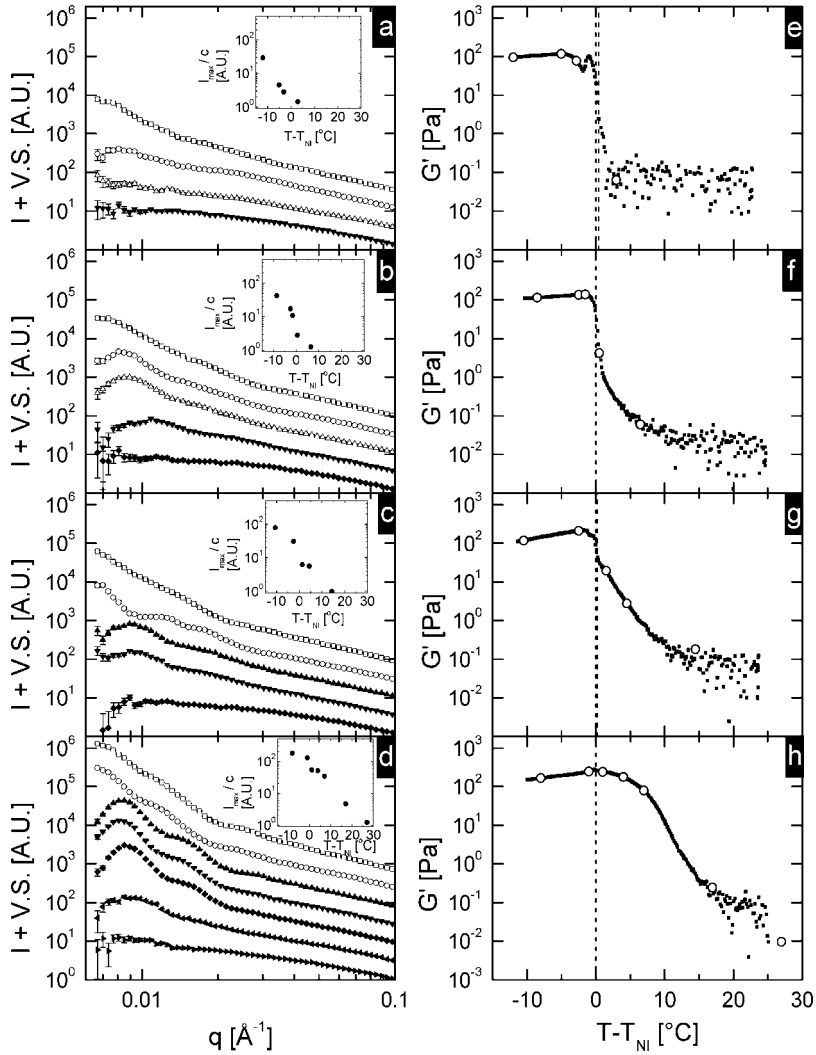

Figure 6. SANS and rheology of 10 wt % diblock copolymer solutions proceeding from top to bottom in order of increasing PS block length. The low-q portion of SANS patterns collected in the nematic phase (open symbols) and the isotropic phase (closed symbols) (a−d) is plotted alongside the storage modulus, $G'(\omega = 10$ rad/s), as a function of temperature upon heating a rate of 1 °C/min (d−h). SANS patterns were collected at the following reduced temperatures: $T - T_{NI}$ = (a) −11.9 °C (□), −4.9 °C (○), −2.9 °C (△), and 3.1 °C (▼); (b) = −8.3 °C (□), −2.3 °C (○), −1.3 °C (△), 0.7 °C (▼), and 6.7 °C (♦); (c) = −10.3 °C (□), −2.3 °C (○), 1.7 °C (▲), 4.7 °C (▼), and 24.7 °C (♦); and (d) = −7.9 °C (□), −0.9 °C (○), 1.1 °C (▲), 4.1 °C (▼), 7.1 °C (♦), 17.1 °C (solid, left-facing triangles), and 27.1 °C (solid, right-facing triangles). Patterns are successively shifted upward from the highest temperature by factors of three for clarity. For parts (d−h), white circles indicate the same reduced temperatures at which SANS patterns were collected, and dashed lines indicate the beginning and end of the nematic−isotropic transition.

micelles,[46] whereas in the latter case, decreased intermicellar interaction yields a substantially lower level of elasticity. Similar to 5 wt % solutions, G' of 10 wt % polymer solutions increases with temperature in the nematic phase (except for the diblock with $M_{PS} = 40$ kg/mol) and decreases with temperature above T_{NI}. However, for $M_{PS} \geq 60$ kg/mol, the decay of G' in the isotropic phase is much more gradual for 10 wt % solutions (cf., Figure 6f−h to Figure 5f−h), in the most extreme case (largest PS block), delaying a 10-fold drop in G' to $T_{NI} +$ 10 °C.

Frequency dependent rheometry of diblock solutions exposes their dynamics as a function of temperature. The magnitude of the complex viscosity, $|\eta^*|$, is normalized by the bulk viscosity of 5CB, η_{5CB}, at the same temperature to remove the solvent's temperature dependence. Solutions of 5 wt % diblocks are viscoelastic fluids in the nematic phase: the reduced viscosity is frequency dependent (Figure 7). In the isotropic phase, the three diblocks with $M_{PS} < 120$ kg/mol lose their viscoelastic character within 5 °C of T_{NI} (i.e., at $T - T_{NI} \geq 5$ °C the reduced viscosity is frequency-independent, Figure 7a−c, characteristic of a viscous fluid). The polymer with the largest PS block remains a viscoelastic fluid up to $T - T_{NI} < 15$ °C (Figure 7d).

When the polymer concentration is increased to 10 wt % the solutions are room-temperature gels (Figure 8, $|\eta^*|/\eta_{5CB} \sim \omega^{-1}$ at the lowest temperature), but the solid-like character is immediately lost when they are heated above T_{NI}. When $M_{PS} = 40$ kg/mol the solution transitions directly to a viscous fluid at T_{NI} (Figure 8a), but when $M_{PS} \geq 60$ kg/mol the solutions remains a viscoelastic fluid up to $T - T_{NI} < 13$ °C (Figure 8b−d).

Within the nematic phase, increasing the size of the PS block increases the longest relaxation times in 10 wt % diblock solutions, manifested by the transition from $|\eta^*|/\eta_{5CB} \sim \omega^{-1}$ to $|\eta^*|/\eta_{5CB} \sim \omega^0$. Solutions of diblocks with $M_{PS} \geq 80$ kg/mol retain $|\eta^*|/\eta_{5CB} \sim \omega^{-1}$ scaling throughout the dynamic range at all temperatures in the nematic phase (Figure 8c,d), that is, the longest relaxation time exceeds the longest experimentally accessible time-scale. When the PS block is decreased to $M_{PS} = 60$ kg/mol, the relaxation time becomes accessible near the isotropization point (deviations from $|\eta^*|/\eta_{5CB} \sim \omega^{-1}$ are observed within 1 °C of T_{NI}, open triangles, Figure 8b). When $M_{PS} = 40$ kg/mol the relaxation time is accessible at still lower temperatures: deviation from $|\eta^*|/\eta_{5CB} \sim \omega^{-1}$ is evident at $T - T_{NI} = -5.3$ °C (Figure 8a).

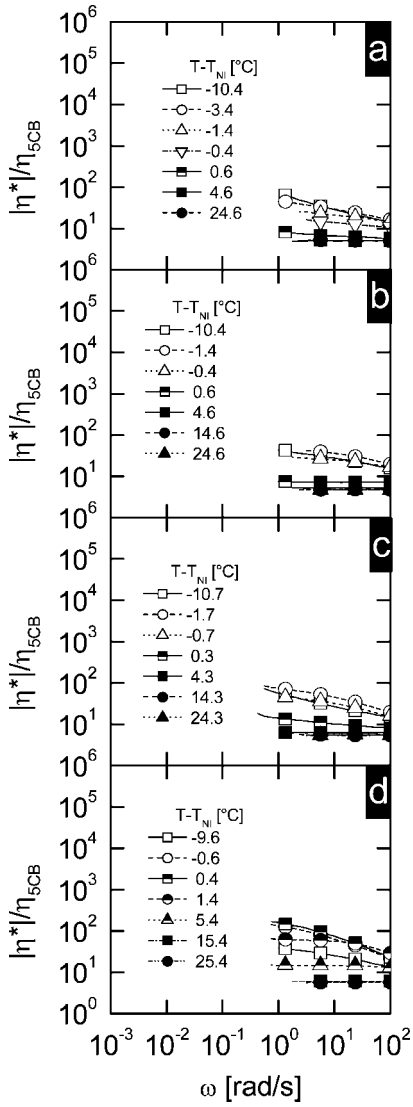

Figure 7. Frequency-dependent rheology of 5 wt % diblock copolymer solutions proceeding from top to bottom in order of increasing PS block length. The reduced complex viscosity, $|\eta^*|/\eta_{5CB}$, is plotted at various temperatures in the nematic phase (open symbols) and the isotropic phase (closed or half-filled symbols). In the isotropic phase half-filled symbols are used to indicate viscoelastic fluids while closed symbols indicate viscous liquids.

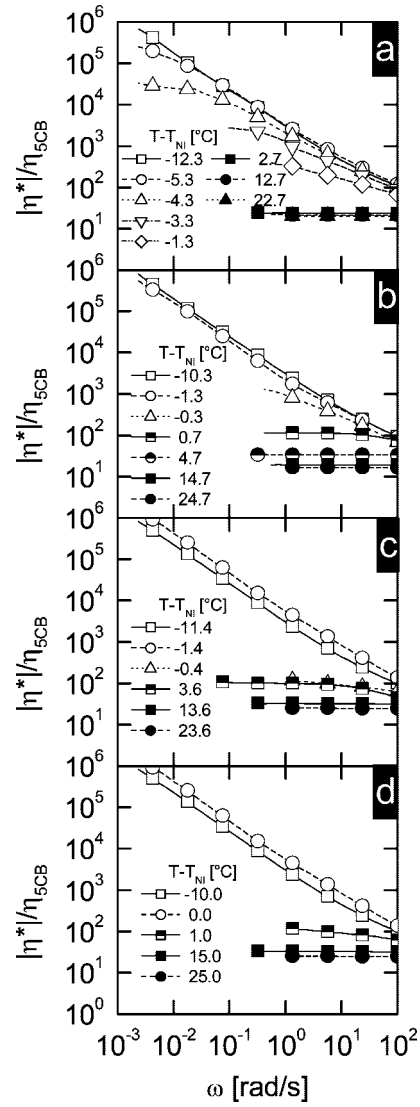

Figure 8. Frequency-dependent rheology of 10 wt % diblock copolymer solutions proceeding from top to bottom in order of increasing PS block length. The reduced complex viscosity, $|\eta^*|/\eta_{5CB}$, is plotted at various temperatures in the nematic phase (open symbols) and the isotropic phase (closed or half-filled symbols). In the isotropic phase half-filled symbols are used to indicate viscoelastic fluids while closed symbols indicate viscous liquids.

Discussion

Heating samples through the nematic−isotropic phase transition has a profound effect on micellar structure and micelle−micelle interactions as a result of the discontinuous change in solvent quality that takes place at T_{NI}. In contrast to conventional solvents, whose quality changes continuously with temperature, the unique ability of the LC solvent to undergo a first-order phase transition between two distinct fluid phases allows the regimes of strong selectivity[5,7,9] and slight selectivity[3,6,8] to be accessed with small changes in temperature. Depending on the copolymer's composition and molecular weight, the temperature at which the micelles disassemble to become free chains (the microphase separation temperature, MST) can be below, above, or coincident with T_{NI}.

The thermodynamic driving forces for self-assembly of coil-SGLCP diblock copolymers may be inferred from the phase behavior of PS and SGLCP homopolymers in 5CB.[12] In the nematic phase, the solvent's orientational order increases the free energy for dissolving PS and renders the polymer insoluble: placing a random-coil polymer in an ordered solvent requires the polymer to adopt an anisotropic conformation and distorts the nematic director field. When these penalties disappear in the isotropic phase, 5CB and PS become miscible. On the other hand, the SGLCP is miscible with 5CB both above and below T_{NI} due to covalent attachment of chemically similar, mesogenic units to the polymer backbone. Self-assembly of coil-SGLCP diblock copolymers below T_{NI} is intuitively understood as being driven by the solvent's strong selectivity for the SGLCP block combined with unfavorable interactions between the polymer blocks. The latter also drives self-assembly in the isotropic phase where the solvent is reasonably good for both blocks.

At fixed total polymer concentration and molecular weight, increasing M_{PS} increases the MST. Interestingly, at short PS block length, the covalent bonding between PS and SGLCP serves to draw the PS block into solution even when the solvent quality for PS is poor; the MST of these solutions (both 5 and 10 wt %) is less than T_{NI}. Increasing the size of the PS block to $M_{PS} = 120$ kg/mol shifts the MST of diblock solutions to be greater than T_{NI}, even though the individual polymers are both miscible with isotropic 5CB. These effects are also evident in

the dynamic rheology: the faster relaxation of micellar solutions with $M_{PS} = 40$ kg/mol than those with $M_{PS} = 120$ kg/mol, is consistent with weaker segregation (shorter characteristic time for chain dissociation from the micellar core).[47,48]

In a given diblock copolymer solution the temperature dependence of G' in the nematic phase may indicate structural changes caused by increased micellar swelling. The rheological properties clearly show micelle-micelle interactions, manifested in viscoelasticity or gelation. In general, the more strongly the micelles interact with one another, the higher G' becomes due to overlap of adjacent coronas.[45,46,49] We envision that PS becomes more compatible with nematic solvent at higher temperatures where the order parameter of 5CB is smaller allowing penetration of solvent into the core. This can lead to changes in aggregation number and overall micelle size, which contribute to raising the elastic modulus (upward slope $G'(T)$ in Figure 5f−h, Figure 6f−h) by increasing the number of micelles and the degree of corona−corona overlap.

The temperature dependence of the elastic modulus through the nematic−isotropic phase transition provides insight into transitions in the self-assembled morphology. For samples that have a substantial G' above T_{NI} (Figure 5h, Figure 6f,h), the temperature-dependence falls into two categories: G' rapidly decreases at T_{NI} (Figure 5h, Figure 6f,g), or G' decreases gradually at first, then rapidly decays after some $T > T_{NI}$ (Figure 6h). The former is characteristic of composition fluctuations that decay above the MST in conventional micellar solutions,[3,8] and the latter indicates that distinct micelles continue to exist in a range of $T_{NI} < T <$ MST, then decay with similar composition fluctuations. These observations are in accord with the scattering patterns that clearly demonstrate the existence of micelles in the temperature range where G' is gradually decreasing (Figure 6d and h), but only show diffuse excess scattering in the range where G' is falling rapidly (Figure 5d and h, Figure 6b and f, Figure 6c and g, Figure 6d and h).

Segregation strength and, consequently, the MST increase with polymer concentration. Unfavorable thermodynamic interactions between the two dissimilar polymer blocks are partially screened in more dilute solutions, but become increasingly dominant as the polymer content is increased. This is evident in the SANS and rheology data of, for example, 10 wt % 320(120)ABSiCB4, which shows that the polymer remains self-assembled up to $T - T_{NI} \approx 7$ °C (Figure 6d and h) but in 5 wt % 320(120)ABSiCB4 the polymer loses its structure just after T_{NI} (Figure 5d and h).

We believe these phenomena are general to coil/SGLCP diblock copolymers in nematic solution: we have performed the same experiments with similar results on an analogous library of diblock copolymers with "side-on" mesogens attached with their long axes parallel to the polymer backbone (see Supporting Information). Subtle differences between the end-on and side-on systems suggests that coupling between liquid crystalline order and polymer conformation may play a role in determining self-assembled morphology, and a focused study of this topic may be of interest in the future.

Conclusions

Compared to conventional diblock copolymers in isotropic solvents, coil/SGLCP diblocks in nematic solvent are thermodynamically rich systems. Solutions of coil-SGLCP diblock copolymers in small-molecule LC solvent are unique in that two distinct regimes of solvent selectivity can be accessed in a single solution, simply by heating the solution through its nematic-to-isotropic phase transition. In the nematic phase, the solvent is strongly selective for the SGLCP block, but in the isotropic phase it is a reasonably good solvent for both blocks. The change in solvent quality often triggers the transition from self-assembled micelles to a solution of free chains, but by tailoring the composition of the block copolymer, the MST can be adjusted to be above or below the T_{NI}.

Acknowledgment. A portion of the results shown in this report are derived from work performed at Argonne National Laboratory. Argonne is operated by UChicago Argonne, LLC, for the U.S. Department of Energy under Contract DE-AC02-06CH11357. Another portion of this work was performed at Oak Ridge National Laboratory's Center for Nanophase Materials Sciences which is sponsored by the Scientific User Facilities Division, Office of Basic Energy Sciences, U.S. Department of Energy. This work benefited from use of the shared facilities supported by the MRSEC Program of the National Science Foundation under Award DMR-0080065. N.R.S., R.V., and J.A.K. acknowledge financial support from the AFOSR LC-MURI (f4962-97-1-0014); S.-Y.P. and J.A.K. acknowledge financial support from MOST and AFOSR NBIT 2007 program. We thank Ed Lang and Zuleika Kurji for assistance with neutron scattering experiments. National Defense Science and Engineering Graduate Fellowships awarded to N.R.S. and R.V. are greatly appreciated.

Supporting Information Available: Table of solution transition temperatures, results from side-on diblock copolymer solutions, and dynamic moduli of end-on diblock copolymer solutions. This material is available free of charge via the Internet at http://pubs.acs.org.

References and Notes

(1) Hamley, I. W. *The Physics of Block Copolymers*; Oxford University Press: Oxford, 1998.
(2) Bates, F. S.; Fredrickson, G. H. *Annu. Rev. Phys. Chem.* **1990**, *41*, 525.
(3) Hamley, I. W.; Fairclough, J. P. A.; Ryan, A. J.; Ryu, C. Y.; Lodge, T. P.; Gleeson, A. J.; Pedersen, J. S. *Macromolecules* **1998**, *31*, 1188.
(4) Hanley, K. J.; Lodge, T. P.; Huang, C.-I. *Macromolecules* **2000**, *33*, 5918.
(5) Lai, C.; Russel, W. B.; Register, R. A. *Macromolecules* **2002**, *35*, 841.
(6) Lodge, T. P.; Hanley, K. J.; Pudil, B.; Alahapperuma, V. *Macromolecules* **2003**, *36*, 816.
(7) Lodge, T. P.; Pudil, B.; Hanley, K. J. *Macromolecules* **2002**, *35*, 4707.
(8) Lodge, T. P.; Xu, X.; Ryu, C. Y.; Hamley, I. W.; Fairclough, J. P. A.; Ryan, A. J.; Pedersen, J. S. *Macromolecules* **1996**, *29*, 5955.
(9) McConnell, G. A.; Gast, A. P. *Macromolecules* **1997**, *30*, 435.
(10) Lodge, T. P.; Blazey, M. A.; Liu, Z. *Macromol. Chem. Phys.* **1997**, *198*, 983.
(11) de Gennes, P.-G. *The Physics of Liquid Crystals*, 2nd ed.; Clarendon Press: Oxford, 1993.
(12) Scruggs, N. R.; Kornfield, J. A.; Lal, J. *Macromolecules* **2006**, *39*, 3921.
(13) Benmouna, F.; Daoudi, A.; Roussel, F.; Buisine, J.-M.; Coqueret, X.; Maschke, U. *J. Polym. Sci., Part B: Polym. Phys.* **1999**, *37*, 1841.
(14) Gogibus, N.; Maschke, U.; Benmouna, F.; Ewen, B.; Coqueret, X.; Benmouna, M. *J. Polym. Sci., Part B: Polym. Phys.* **2001**, *39*, 581.
(15) Scruggs, N. R.; Kornfield, J. A. *Macromol. Chem. Phys.* **2007**, *208*, 2242.
(16) Benthack-Thoms, H.; Finkelmann, H. *Makromol. Chem.* **1985**, *186*, 1895.
(17) Brochard, F.; Jouffroy, J.; Levinson, P. *J. Phys. (Paris)* **1984**, *45*, 1125.
(18) Casagrande, C.; Veyssie, M.; Finkelmann, H. *J. Phys. (Paris)* **1982**, *43*, L671.
(19) Chiu, H.-W.; Kyu, T. *J. Chem. Phys.* **1995**, *103*, 7471.
(20) Chiu, H.-W.; Zhou, Z. L.; Kyu, T.; Cada, L. G.; Chien, L.-C. *Macromolecules* **1996**, *29*, 1051.
(21) Kihara, H.; Kishi, R.; Miura, T.; Kato, T.; Ichijo, H. *Polymer* **2001**, *42*, 1177.
(22) Sigaud, G.; Achard, M. F.; Hardouin, F.; Coulon, C.; Richard, H.; Mauzac, M. *Macromolecules* **1990**, *23*, 5020.
(23) Sigaud, G.; Achard, M. F.; Hardouin, F.; Mauzac, M.; Richard, H.; Gasparoux, H. *Macromolecules* **1987**, *20*, 578.
(24) ten Bosch, A.; Maissa, P.; Sixou, P. *J. Chem. Phys.* **1983**, *79*, 3462.
(25) Mao, G.; Ober, C. K. *Acta Polym.* **1997**, *48*, 405.
(26) Sanger, J.; Gronski, W.; Leist, H.; Wiesner, U. *Macromolecules* **1997**, *30*, 7621.

(27) Sanger, J.; Gronski, W.; Maas, S.; Stuhn, B.; Heck, B. *Macromolecules* **1997**, *30*, 6783.
(28) Anthamatten, M.; Wu, J.-S.; Hammond, P. T. *Macromolecules* **2001**, *34*, 8574.
(29) Hamley, I. W.; Castelletto, V.; Lu, Z. B.; Imrie, C. T.; Itoh, T.; Al-Hussein, M. *Macromolecules* **2004**, *37*, 4798.
(30) Zheng, W. Y.; Hammond, P. T. *Macromolecules* **1998**, *31*, 711.
(31) Walther, M.; Bohnert, R.; Derow, S.; Finkelmann, H. *Macromol. Rapid Commun.* **1995**, *16*, 621.
(32) Walther, M.; Faulhammer, H.; Finkelmann, H. *Macromol. Chem. Phys.* **1998**, *199*, 223.
(33) Walther, M.; Finkelmann, H. *Macromol. Rapid Commun.* **1998**, *19*, 145.
(34) Schneider, A.; Müller, S.; Finkelmann, H. *Macromol. Chem. Phys.* **2000**, *201*, 184.
(35) Kempe, M. D.; Scruggs, N. R.; Verduzco, R.; Lal, J.; Kornfield, J. A. *Nat. Mater.* **2004**, *3*, 177.
(36) Kempe, M. D.; Verduzco, R.; Scruggs, N. R.; Kornfield, J. A. *Soft Matter* **2006**, *2*, 422.
(37) Verduzco, R.; Meng, G.; Kornfield, J. A.; Meyer, R. B. *Phys. Rev. Lett.* **2006**, *96*, 147802.
(38) Verduzco, R.; Scruggs, N. R.; Sprunt, S.; Palffy-Muhoray, P.; Kornfield, J. A. *Soft Matter* **2007**, *3*, 993.
(39) Hadjichristidis, N.; Iatrou, H.; Pispas, S.; Pitsikalis, M. *J. Polym. Sci., Part A: Polym. Chem.* **2000**, *38*, 3211.
(40) Morton, M.; Fetters, L. *J. Rubber Chem. Technol.* **1975**, *48*, 359.
(41) Uhrig, D.; Mays, J. W. *J. Polym. Sci., Part A: Polym. Chem.* **2005**, *43*, 6179.
(42) Wu, S. T.; Wang, Q. H.; Kempe, M. D.; Kornfield, J. A. *J. Appl. Phys.* **2002**, *92*, 7146.
(43) Holmqvist, P.; Fytas, G.; Pispas, S.; Hadjichristidis, N.; Saijo, K.; Tanaka, H.; Hashimoto, T. *Macromolecules* **2004**, *37*, 4909.
(44) McConnell, G. A.; Gast, A. P.; Huang, J. S.; Smith, S. D. *Phys. Rev. Lett.* **1993**, *71*, 2102.
(45) Watanabe, H.; Kotaka, T. *J. Rheol.* **1983**, *27*, 223.
(46) Watanabe, H. *Acta Polym.* **1997**, *48*, 215.
(47) Tanaka, F. *Polym. J. (Tokyo, Jpn.)* **2002**, *34*, 479.
(48) Tanaka, F. *JSME Int. J., Ser. B* **2002**, *45*, 123.
(49) Watanabe, H.; Kanaya, T.; Takahashi, Y. *Macromolecules* **2001**, *34*, 662.

MA801598Y